

Magnetic resonance imaging patterns of treatment-related toxicity in the pediatric brain: an update and review of the literature

Maria Camilla Rossi Espagnet¹ · Luca Pasquini^{1,2} · Antonio Napolitano³ · Antonella Cacchione⁴ · Angela Mastronuzzi⁴ · Roberta Caruso⁴ · Paolo Tomà⁵ · Daniela Longo¹

Received: 30 May 2016 / Revised: 23 September 2016 / Accepted: 2 November 2016 / Published online: 9 December 2016
© Springer-Verlag Berlin Heidelberg 2016

Abstract Treatment-related neurotoxicity is a potentially life-threatening clinical condition that can represent a diagnostic challenge. Differentiating diagnoses between therapy-associated brain injury and recurrent disease can be difficult, and the immediate recognition of neurotoxicity is crucial to providing correct therapeutic management, ensuring damage reversibility. For these purposes, the knowledge of clinical timing and specific treatment protocols is extremely important for interpreting MRI patterns. Neuroradiologic findings are heterogeneous and sometimes overlapping, representing the compounding effect of the different treatments. Moreover, MRI patterns can be acute, subacute or delayed and involve different brain regions, depending on (1) the mechanism of action of the specific medication and (2) which brain regions are selectively vulnerable to specific toxic effects. This review illustrates the most common radiologic appearance of

radiotherapy, chemotherapy and medication-associated brain injury in children, with special focus on the application of advanced MRI techniques (diffusion, perfusion and proton spectroscopy) in the diagnosis of the underlying processes leading to brain toxicity.

Keywords Adverse effects · Anti-neoplastic therapy · Brain · Children · Magnetic resonance imaging · Neuroradiology · Toxicity

Introduction

The term “treatment-related neurotoxicity” encompasses a heterogeneous group of clinical conditions in which the causative agent is an exogenous factor that may be identified in a specific medication or treatment protocol administered to the patient. Most literature reviews on this topic cover the adult population and only a few studies address the pediatric brain, with the most recent ones focusing on one specific medication-related toxicity, or on a specific group of patients [1–5].

With the recent advances in treatment protocols, especially in the fields of oncology and hematology, the recognition of neurotoxic patterns of injury in children is becoming a diagnostic challenge. In this population, differentiating diagnoses between therapy-associated brain injury and recurrent disease is crucial for the child’s therapeutic management and it requires prompt identification to help ensure damage reversibility and to avoid unnecessary aggressive treatments.

Specific medication-associated neurotoxicities sometimes manifest clinically as an urgent acute neurological condition, often requiring a prompt diagnostic and therapeutic management. This is especially true for neonates, where neurological

✉ Maria Camilla Rossi Espagnet
camilla.rossiespagnet@gmail.com

¹ Neuroradiology Unit, Department of Imaging
Bambino Gesù Children’s Hospital, IRCCS
Piazza S. Onofrio 4, 00165 Rome, Italy

² NESMOS Department
Sant’ Andrea Hospital, Sapienza University
Via di Grottarossa 1035, Rome, Italy

³ Enterprise Risk Management, Medical Physics Department
Bambino Gesù Children’s Hospital, IRCCS
Rome, Italy

⁴ Department of Hematology/Oncology and Stem Cell Transplantation
Bambino Gesù Children’s Hospital, IRCCS
Rome, Italy

⁵ Department of Imaging
Bambino Gesù Children’s Hospital, IRCCS
Rome, Italy

symptoms are sometimes nonspecific, and the complex spectrum of endogenous toxic injuries, such as metabolic disorders, can confound the differential diagnosis [6].

Medical progress has led to an improvement of survival rates in children affected by either hematologic diseases or brain tumors, thus increasing the observation of delayed treatment-related effects [7]. A 4-fold increase in risk of severe health conditions has been reported in adult survivors of childhood leukemia compared to siblings of cancer survivors [8], and survivors treated with cranial radiotherapy seem to be at the greatest risk of metabolic, endocrine and neuro-cognitive dysfunction [9].

The known mechanisms of action of the most common therapeutic agents might explain the MRI patterns of toxicity-related injury because of the vulnerability of specific brain structures, the so-called topistic areas such as deep gray matter nuclei, which are often involved symmetrically and bilaterally in treatment-induced injury by various pharmacological agents [6, 10].

However when complex treatment protocols are applied, the radiologic picture can remain nonspecific, and only a combined knowledge of treatment-associated neurological adverse effects and of their clinical timing can help define possible diagnoses.

The purpose of this review is to describe specific clinical and radiologic scenarios of toxic encephalopathy, particularly the effects of radio-chemotherapy for solid tumors or myelo-proliferative disorders, and of anti-epileptic and antibiotic medications. In this review we focus on the application of specific MRI techniques (diffusion, perfusion and proton spectroscopy).

In this paper we classify clinical conditions on the basis of their associated therapeutic agent (Fig. 1). However considering the heterogeneity of treatment protocols for pediatric oncologic-hematologic patients, all neurotoxic patterns should be considered as a part of possible overlapping scenarios,

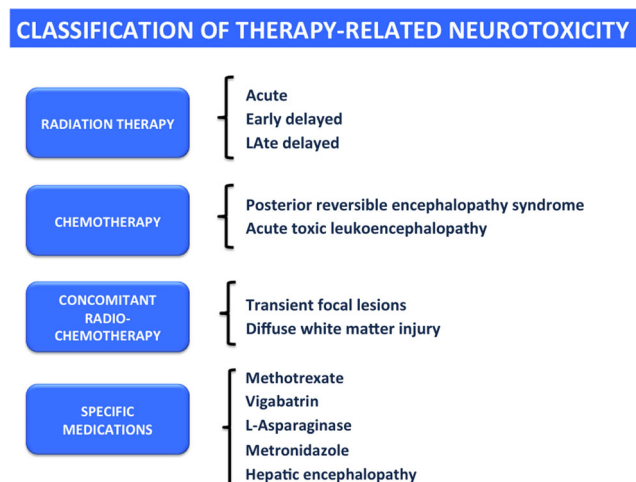


Fig. 1 Classification of therapy-related patterns of neurotoxicity

taking into account the possible compounding toxic effects of multiple therapeutic agents.

Radiotherapy

The effects of brain radiation depend on several factors, such as patient age, cumulative irradiation dose, type of irradiation (i.e. accelerated, conformal, hyperfractionated), duration of exposure, and concomitant antineoplastic or radiosensitizing agents. The classification of radiation effects on the brain is based on timing of the clinical presentation, and is divided into three main categories: acute (within 1–6 weeks), subacute or early delayed (3 weeks to 6 months) and chronic or late delayed (6 months to years) [2, 11]. Here we will only examine subacute and chronic effects, because acute effects are rare and often asymptomatic.

Early delayed effects

Early delayed effects represent the least understood injury from brain irradiation, and these effects occur between 3 weeks and several months after therapy. Transient demyelination is considered to be the underlying pathological process, and this is radiologically characterized by diffuse increased signal intensity on T2-weighted MR images within the white matter, more often periventricular (Fig. 2). These children are often clinically asymptomatic or present with mild attention deficit or sleepiness, and the clinical course is usually benign, with spontaneous resolution [2].

Late delayed effects — radiation necrosis

Late delayed effects of radiotherapy include a wide spectrum of brain injuries that mainly depend on the therapeutic approach (i.e. whole brain, stereotactic or 3-D conformal radiation) and on the variety of underlying physiopathological mechanisms involving vascular-related injury and direct effects on brain parenchyma, with a significant vulnerability of the white matter [12]. Consequently neuroimaging patterns are variable, ranging from the absence of visible macroscopic brain damage (usually associated with fractionated whole-brain irradiation) to frank focal areas of parenchymal necrosis that can occur 3–12 months after treatment (this more often occurs with administration of fractionated therapy in a selected region) [2, 11].

Radiation necrosis is defined as a severe focal tissue reaction characterized by blood–brain barrier disruption, and vasogenic edema and necrosis, with or without mass effect on MRI [12, 13]. The exact incidence and risk factors of radiation necrosis in children undergoing cranio-spinal irradiation remain undetermined because most reports on this condition refer to the adult population. However a large study on

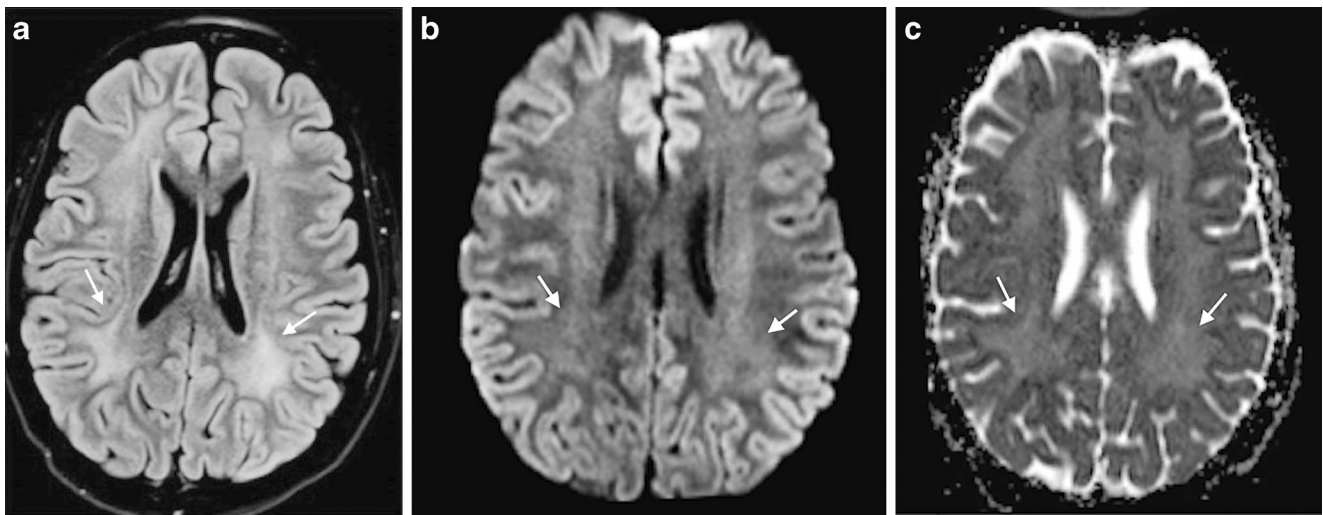


Fig. 2 Early delayed pattern of radiotherapy in a 15-year-old girl who had lymphoblastic lymphoma treated with whole-brain radiotherapy. **a** Axial FLAIR MR sequence (TR/TE/TI = 9,000/85/500 ms, flip angle = 150°) demonstrates diffuse hyperintense signal symmetrically involving periventricular white matter (arrows). **b**, **c** Axial diffusion-

weighted imaging (DWI) sequence (TR/TE = 9,000/98 ms, b values = 0, 1,000) (**b**) and corresponding apparent diffusion coefficient (ADC) map (**c**) demonstrate absence of diffusion restriction (arrows). The girl fully recovered without any specific treatment. FLAIR fluid-attenuated inversion recovery, TE echo time, TI inversion time, TR repetition time

236 children affected by central nervous system embryonal tumors treated with chemotherapy and cranio-spinal irradiation reported a cumulative incidence of radiation necrosis of about 3.7% at 5 years, with a higher incidence in patients affected by infratentorial tumors [14]. As reported in the literature, risk factors for radiation necrosis include clinical factors (tumor extent, surgical morbidity and postoperative central nervous system infection), percentage of infratentorial brain receiving radiation doses >50 Gy, and adjuvant chemotherapy. The clinical course of radiation necrosis may be variable, ranging from asymptomatic presentation to focal mild neurological symptoms, including seizures and cranial nerve deficits, to death in the most severe scenarios [14].

Although the diagnostic reference standard for radiation necrosis diagnosis is biopsy, MRI can assist in the diagnosis through a combination of conventional MR sequences with advanced techniques, such as (dynamic susceptibility contrast-enhanced) perfusion imaging and MR spectroscopy.

On conventional imaging the MR pattern of radiation necrosis usually shows, at a distance from the primary tumor site, a T2 hyperintense lesion with or without mass effect, surrounding vasogenic edema and heterogeneous contrast enhancement, described by Kumar et al. [15] as a “Swiss cheese” or “soap bubble” pattern (Fig. 3).

Perfusion images of radiation necrosis usually show absence of elevated perfusion on relative cerebral blood volume maps compared to recurrent tumor, suggesting ischemia-related changes and iatrogenic vasculopathy [13, 16, 17] (Fig. 3). However a clear differentiation between the entities is not always possible at radiologic examination because they sometimes coexist within the same lesion and standardized relative cerebral blood volume-cutoff values have not been

established to clearly distinguish the two entities [18–20]. MR spectroscopy is another tool to examine the suspected necrosis; it demonstrates high lipid and lactate peaks with variable concentrations of choline, N-acetylaspartate and creatine [21].

However to differentiate radiation necrosis from recurrent tumor, a thorough evaluation of serial changes on follow-up examinations is also crucial because the resolution of necrotic changes may be a long process, entailing various combinations of reduction or enlargement of necrotic lesions before complete stabilization [14].

In the last decade an increasing number of hospitals worldwide have installed systems for proton beam therapy. The main advantage of this technique over conventional photon therapy is the reduction of the dose to normal tissues, which can be achieved through more precise control of the proton beam depth. Specific guidelines for the use of proton therapy in pediatric central nervous system tumors have been developed but its use in clinical practice is still limited because of its insufficient availability [22]. For these reasons studies of possible proton-therapy-induced neurotoxicity are still scarce.

Late delayed effects — other

Children treated with cranial irradiation develop a higher risk of hormonal disturbances as a result of an impaired hypothalamic-pituitary axis, as well as brain atrophy, calcifications, vascular malformations and secondary malignancies [5].

Secondary cerebral cavernous malformations have been reported as the most frequent MRI abnormalities in childhood leukemia survivors treated with cranial radiotherapy, with an

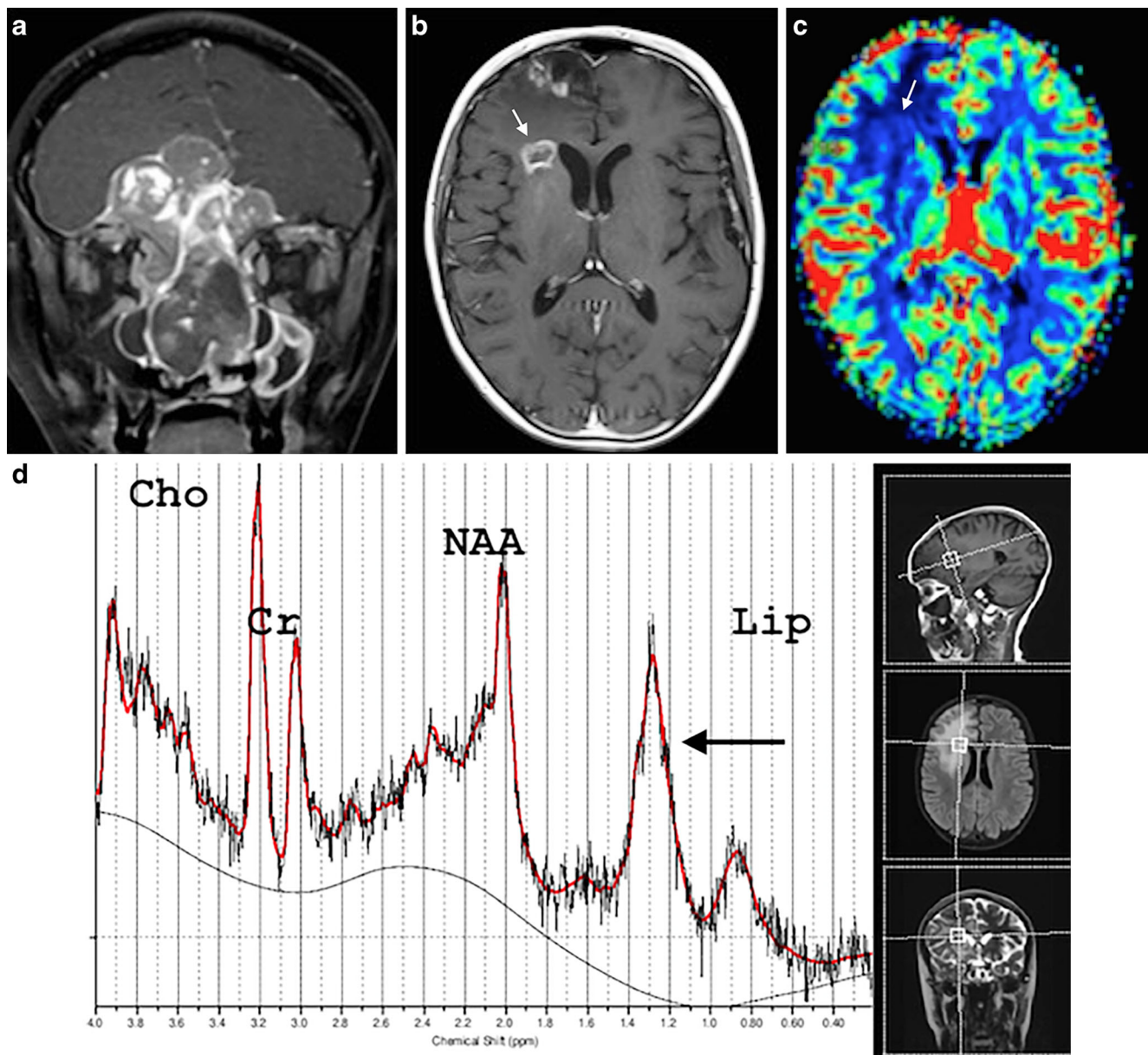


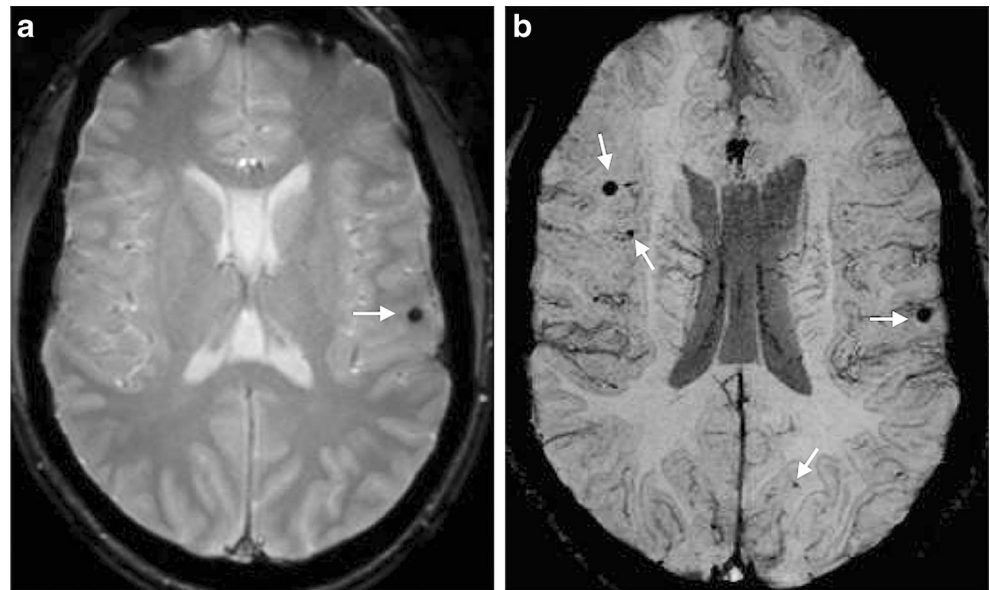
Fig. 3 Radiation necrosis in a 12-year-old girl who had Ewing sarcoma of the ethmoid sinus treated with high-dose chemotherapy and radiotherapy. **a** Coronal post-contrast T1-weighted MR sequence with fat saturation (TR/TE = 500/9.9 ms, flip angle = 75°) demonstrates a huge lesion bilaterally involving the sinusal cavity and extending upward to the anterior cranial fossa. **b** Axial post-contrast T1-weighted MR sequence (TR/TE = 500/9.9 ms, flip angle = 75°) 1 year after treatment initiation shows areas of focal irregular contrast enhancement within the anterior right frontal lobe and the periventricular white matter (*arrow*). **c** Cerebral blood volume (CBV) map from dynamic

susceptibility contrast-enhanced (DSC) perfusion technique (TR/TE = 1,860/30 ms, flip angle = 90°) does not show areas of increased perfusion (*arrow*). **d** Proton MR spectroscopy water-suppressed proton spectra recorded with a stimulated echo acquisition mode pulse sequence (TR/TE = 1,500/30 ms; acquisitions = 96) of a voxel located in the periventricular lesion demonstrates a reduction of N-acetylaspartate (NAA, 2.0 ppm) concentration with mild choline (Cho, 3.2 ppm) elevation and a lipid peak (Lip, 1.3 ppm, *arrow*), suggesting the diagnosis of radiation necrosis, *Cr* creatine, *TE* echo time, *TR* repetition time

incidence of 57% [23]. Several studies have described a higher incidence of cerebral cavernous malformations in the periphery of the radiation field, suggesting a more effective role of low radiation doses compared to higher doses in the genesis of these secondary vascular malformations [24]. Cerebral cavernous malformations detection increases with the acquisition of T2*-weighted gradient-echo MR sequences

and susceptibility-weighted images, which have a higher sensitivity in identifying susceptibility effects of blood product deposits [25] (Fig. 4). Clinical presentations of cerebral cavernous malformations can be heterogeneous, varying from asymptomatic conditions to seizures or rare fatal hemorrhage, which is believed to occur with a higher incidence when cerebral cavernous malformations are located in deep cerebral

Fig. 4 Multiple cerebral cavernous malformations secondary to radiotherapy in a 26-year-old man who survived childhood acute lymphoblastic leukemia. **a** Axial T2* gradient echo sequence (TR/TE = 600/6.2 ms, flip angle = 136°) demonstrates susceptibility artifact (*arrow*). **b** Abnormalities are better depicted on axial susceptibility-weighted imaging (TR/TE = 28/20 ms, flip angle = 15°) in bilateral juxtacortical brain regions (*arrows*), suggestive of secondary cerebral cavernous malformations. *TE* echo time, *TR* repetition time



structures [26]. However the differences in clinical history between radiation-induced cerebral cavernous malformations and isolated ones have not been fully elucidated: some studies have attributed to the former a lower incidence of seizures, while others have reported in the same group a higher occurrence of hemorrhagic events [27, 28]. Therefore surgical treatment should be considered only in select cases presenting with refractory seizures, and recurrent hemorrhage or neurological deterioration [26].

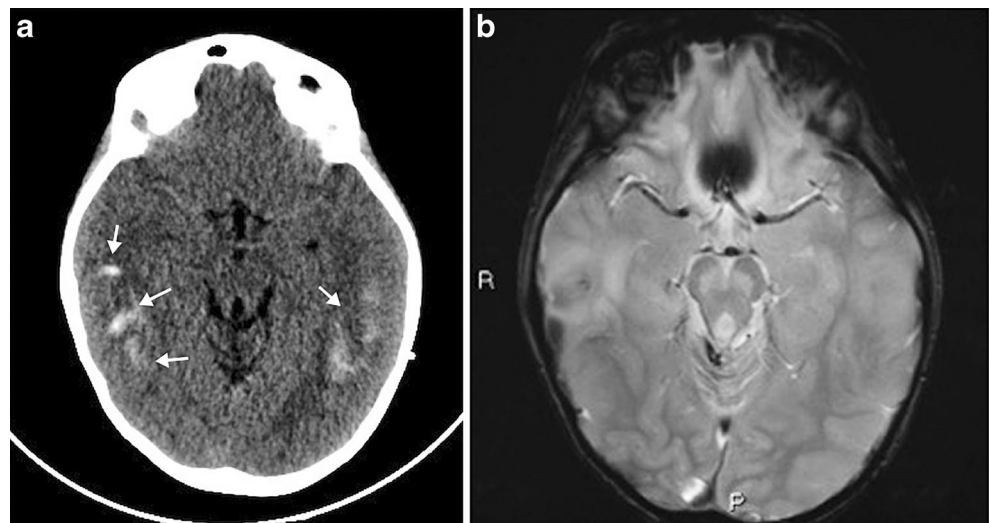
Mineralizing microangiopathy is a well-known form of radiation-induced damage, resulting from injury to small- and medium-size vessels with hyalinization, fibrinoid necrosis, endothelial proliferation and calcium deposition. The best diagnostic radiologic tool for mineralizing microangiopathy is CT, which shows calcium deposition mainly localized in the basal ganglia and subcortical white matter [4, 29] (Fig. 5).

Secondary brain tumors are a severe complication of cranial irradiation and have been reported with a variable cumulative incidence ranging from 4% to 15% depending on the duration of follow-up. These lesions are mainly represented by meningiomas, which, compared to the primary tumors, are reported to have a more aggressive course and a higher incidence of recurrence [30, 31].

Chemotherapy

Chemotherapy-related neurotoxicity in children is a rare condition, and it often presents clinically with acute severe neurological symptoms. The main chemotherapeutic agents associated with central nervous system toxic effects are

Fig. 5 Radiation-induced-mineralizing angiopathy in an 8-year-old boy treated with radiotherapy and chemotherapy for cerebellar ependymoma. **a** Axial CT image demonstrates bilateral subcortical hyperdensities (*arrows*). **b** Corresponding abnormalities are not clearly visible on MR axial T2* gradient echo sequence (TR/TE = 600/6.2 ms, flip angle = 136°), suggesting mineralizing microangiopathy. *TE* echo time, *TR* repetition time



methotrexate, cytarabine, vincristine, asparaginase and corticosteroids [5]. Clinical and radiologic patterns can be extremely heterogeneous because of the vast variety and combinations of medications. However, considering their clinical relevance and prevalence, we focus here on the most commonly observed forms of toxic leukoencephalopathy associated with chemotherapeutic agent administration or immunosuppression, namely posterior reversible encephalopathy syndrome and acute toxic leukoencephalopathy.

Posterior reversible encephalopathy syndrome

Posterior reversible encephalopathy syndrome (PRES) is a clinical condition characterized by headache, seizures, visual disorders and altered mental status. In children, PRES is not a rare disorder and it can develop during oncologic treatment for hematologic diseases and solid tumors, especially during the induction phase of treatment or, more often, during transplantation-associated immunosuppressive therapy (cyclosporine and tacrolimus) [32, 33]. Several pathological conditions in pediatric patients with PRES have been described, namely infections or sepsis, post-transplantation immunosuppressive therapy, and post-chemotherapy and autoimmune disorders [33].

The exact pathiopathogenic mechanism of the disorder is not fully understood. Two main theories have been proposed and both are supported by contrasting findings in the literature. In the original theory, cerebral hypoperfusion with subsequent vasogenic edema is the endpoint of a vasoconstrictive response that is thought to be an attempt to compensate for evolving hypertension. A more recent theory suggests that severe hypertension exceeding vascular autoregulation limits is the pivotal event leading to hyperperfusion with subsequent blood–brain barrier injury and brain edema [34]. This hypothesis has been recently supported by a report on postoperative PRES in a child treated for posterior fossa tumor; in this case PRES was caused by intraoperative hypertension following brainstem manipulation [35].

In case of treatment with cyclosporine, the pathogenic mechanism seems to depend on direct endothelial damage caused by the specific therapeutic agent that determines a cytokine storm with subsequent increased systemic blood pressure, induced sympathetic autoregulatory vasoconstriction, and breakdown of physiological autoregulation. In turn, these events lead to cerebral hypoperfusion, blood–brain barrier damage and vasogenic edema [34].

Posterior territory involvement is more common than anterior territory involvement. This is thought to be related to sparse sympathetic innervation of the vertebrobasilar circulation, which makes this territory more vulnerable to altered autoregulation response in PRES [36].

In the pediatric setting, PRES is often associated with immunosuppressive agents, like cyclosporine and tacrolimus, for

allogenic bone marrow transplantation in children affected by hematopoietic malignancies [37]. Cyclosporine neurotoxicity is considered to occur in 7–9% of all allogenic bone marrow transplantation [32], while tacrolimus-related PRES is responsible for 1.6% of all PRES cases with a clinical onset after 61 days from treatment initiation [36]. Both neurotoxic syndromes seem to be unrelated to dose and a prompt treatment discontinuation is usually followed by clinical improvement.

In most children with PRES, hypertension has been identified as a predisposing condition often triggered by corticosteroid therapy or renal dysfunction. However, 20–40% of patients are normotensive at the time of clinical onset [37]. Other triggers, especially identified on leukemic patients, include tumor lysis syndrome, which may induce acute renal failure and electrolytic disequilibrium, leading to PRES development.

The MRI pattern is usually characterized by vasogenic edema with increased signal on T2-weighted images, and apparent diffusion coefficient maps without contrast enhancement. Signal alterations most commonly affect parietal and occipital lobes, but frontal lobes and cerebellum can also be involved, especially in children (Fig. 6) [38]. Therefore recent studies tend to consider PRES a misnomer because this syndrome is not always posterior nor always reversible. In both children and adults, hemorrhage and diffusion restriction might be observed and are often related to irreversible brain damage; on the other hand, contrast enhancement caused by blood–brain barrier breakdown is more commonly reported in the pediatric population [37, 38].

Acute toxic leukoencephalopathy

Acute toxic leukoencephalopathy is a form of white matter damage with acute neurological symptoms that can be caused by a wide spectrum of exogenous or endogenous toxic insults, ranging from chemotherapeutic agents (e.g., methotrexate, 5-fluorouracil, fludarabine) and immunosuppressive agents (e.g., cyclosporine, tacrolimus) to environmental toxins (e.g., carbon monoxide) and congenital metabolic disorders. Clinical scenarios vary from completely reversible symptoms to severe neurological damage, depending on the primary cause of the acute toxic leukoencephalopathy, with hypoxic–ischemic injury and endogenous metabolic disorders being associated with neurologic sequelae, and exogenous toxins being more often related to reversible clinical conditions [39, 40].

However, even though the clinical prognosis of acute toxic leukoencephalopathy is extremely heterogeneous, the underlying causes share two common features: the combination of acute neurological symptoms with a common MRI pattern of disease.

The MRI pattern is characterized by symmetrical and bilateral signal alterations in the white matter of centrum

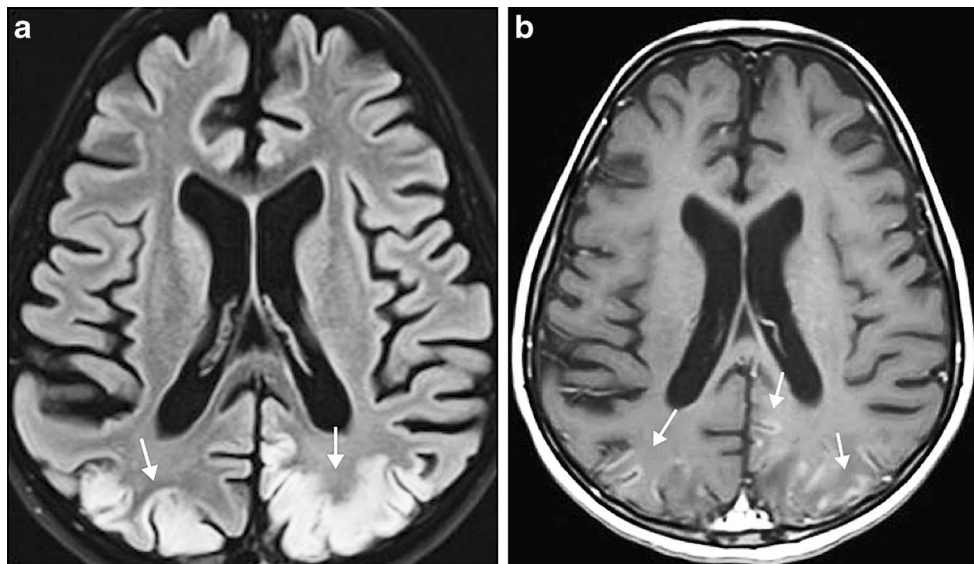


Fig. 6 Posterior reversible encephalopathy syndrome (PRES) in a 10-year-old boy who had hemophagocytic lymphohistiocytosis and was undergoing cyclosporine therapy. **a** Axial FLAIR sequence (TR/TE/TI = 9,000/85/500 ms, flip angle = 150°) demonstrates diffuse hyperintensities involving occipito-parietal cortical and subcortical

regions (arrows). **b** There is corresponding mild contrast enhancement with gyral pattern (arrows) on axial T1-weighted sequence (TR/TE = 500/9.9 ms, flip angle = 75°) after gadolinium administration. FLAIR fluid-attenuated inversion recovery, TE echo time, TI inversion time, TR repetition time

semiovale and corona radiata, which are hyperintense on T2-weighted sequences. This pattern typically shows restricted diffusion on early imaging, suggesting cytotoxic edema, and it usually lacks contrast enhancement (Fig. 7).

Because acute toxic leukoencephalopathy is rarely biopsied as a result of its clinical reversibility, the pathogenesis is poorly understood and probably multifactorial. In the treatment-related setting, the suggested mechanisms of

toxicity include direct microvasculature damage or an excitotoxic effect on the tissue [41, 42].

The main differential diagnosis of acute toxic leukoencephalopathy in the pediatric population includes PRES because of its acute neurological-related manifestations and common clinical oncologic–hematologic setting.

Compared to PRES, acute toxic leukoencephalopathy has similar clinical symptoms at onset, mainly consisting of

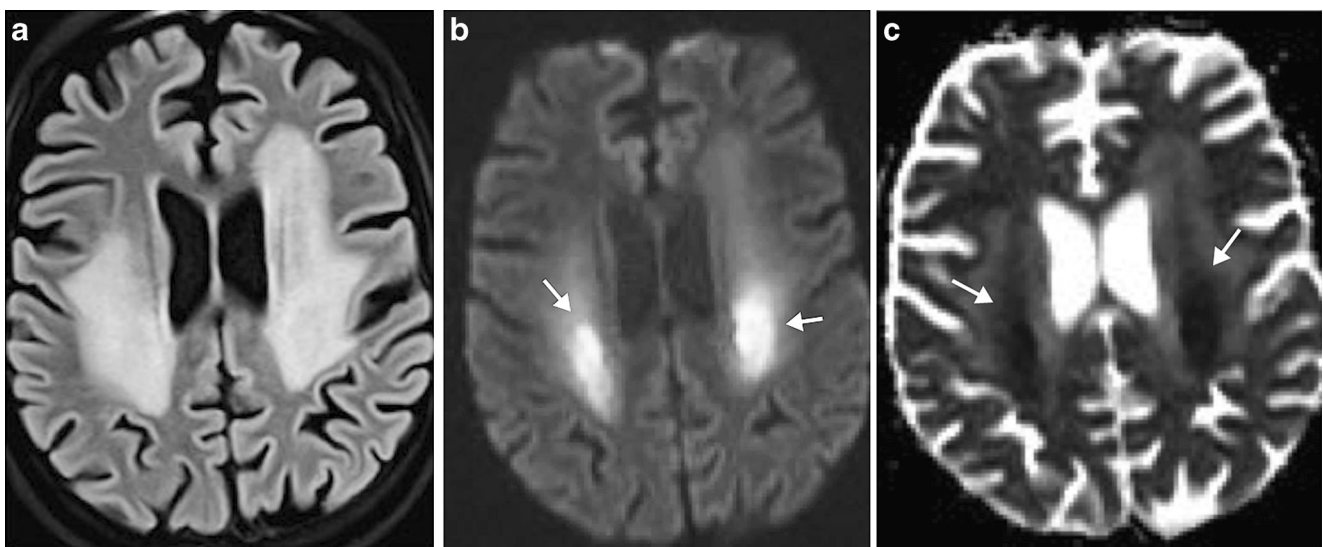


Fig. 7 Acute toxic leukoencephalopathy in a 17-year-old girl with acute lymphoblastic leukemia treated with high-dose chemotherapy and intrathecal methotrexate. **a** Axial FLAIR sequence (TR/TE/TI = 9,000/85/500 ms, flip angle = 150°) demonstrates bilateral symmetrical areas of hyperintense signal symmetrically involving periventricular white

matter. **b, c** There is corresponding diffusion restriction on axial (b) diffusion-weighted imaging (TR/TE = 9,000/98 ms, b value = 1,000; arrows) and (c) apparent diffusion coefficient map (b values = 0, 1,000; arrows). FLAIR fluid-attenuated inversion recovery, TE echo time, TI inversion time, TR repetition time

headache, seizures, visual impairment and altered cognition, but, differently from PRES, in acute toxic leukoencephalopathy cognitive dysfunction might be more severe. Moreover MRI lesion distribution is often different in the two disorders, being more commonly located in the cortex or subcortical white matter in PRES and in the deep white matter in acute toxic leukoencephalopathy [3]. Finally, the prognosis of acute toxic leukoencephalopathy is slightly worse than that of PRES, and the clinical severity is most commonly related to the extent of MRI findings [43].

Concomitant chemo/radiotherapy

The risk of developing central nervous system complications increases when chemotherapy is associated with brain irradiation, suggesting a possible additive role of chemotherapeutic agents to radiation in determining a toxic effect.

In the last few years, new therapeutic protocols for the treatment of malignant pediatric brain tumors, such as primitive neuroectodermal tumors and medulloblastomas, have been introduced to improve overall survival. The recently introduced therapeutic strategies for metastatic medulloblastomas combine the use of high-dose chemotherapy and hyperfractionated accelerated radiotherapy with myeloablative doses of thiotepa in select high-risk cases [44].

The improvement of overall survival in metastatic medulloblastomas treated with the aforementioned protocol (often referred to as the Milan protocol) is still a matter of debate because only single-center studies with conflicting results are available [44, 45]. However these therapeutic strategies, and especially the combination of radiotherapy with thiotepa, have increased the observation of different patterns of neurotoxicity, namely transient white matter lesions (also referred to as transient focal enhancing lesions) and diffuse white matter injury [46, 47].

Transient focal enhancing lesions

Transient focal enhancing lesions have been recently observed in patients treated with radiotherapy (especially hyperfractionated accelerated radiotherapy) and high-dose chemotherapy with myeloablative doses of thiotepa for the treatment of primary malignant central nervous system tumors, and have been associated with both symptomatic and asymptomatic clinical conditions [46–48]. Transient focal enhancing lesions can occur about 7–8 months after chemotherapy/radiotherapy initiation, either in supra- or infratentorial regions, but they most frequently involve the pons and cerebellum in locations remote from the primary tumor site [47].

MRI appearance consists of focal millimetric lesions isointense to gray matter on T1-weighted sequences and hyperintense on T2-weighted sequences, almost always showing avid nodular (described as “snowflakes”) or curvilinear contrast enhancement [46].

Diffusion-weighted imaging can be helpful to differentiate transient focal enhancing lesions from recurrent disease, showing increased diffusion in transient focal enhancing lesions compared to recurrence, and diffusion restriction in recurrence [47]. However this is not always true because diffusion restriction has also been described in transient focal enhancing lesions. Moreover, not all medulloblastomas show low apparent diffusion coefficient values [47]. These considerations are even more important when the two conditions coexist.

In the majority of patients, these lesions resolve spontaneously within a variable period of time, but they may also remain stable or progress to atrophy or radiation necrosis [46] (Fig. 8). The pathogenesis of this neurotoxic phenomenon is poorly understood, but authors suggest that a compounding toxic effect of radiation with chemotherapy or thiotepa, together with an immune reaction after autologous stem cell transplant, might play a pivotal role [46]. The few pathologically proven samples available have shown the presence of diffuse demyelination within the white matter lesions, without evidence of significant inflammation [48].

Diffuse white matter injury

Concomitant administration of chemotherapy and irradiation for both solid and hematologic central nervous system tumors has been associated with a diffuse form of white matter injury, often referred to as leukoencephalopathy. About 80% of patients treated for acute lymphoblastic leukemia develop leukoencephalopathy, and the improved overall survival of patients affected by primary brain tumors has led to a higher recognition of this entity in this category of patients [7].

Risk factors associated with the development of leukoencephalopathy are higher radiation doses, methotrexate administration, and younger age of the patient, the last of which is probably related to a great vulnerability of the myelinating brain to toxicity [7, 49].

Neurological signs vary from subtle progressive cognitive deterioration to severe neurological disturbances. Similarly, MRI pattern is characterized by transient soft non-enhancing periventricular T2-hyperintensities to slowly progressive confluent analogous signal alterations, which follow a centrifugal pattern from periventricular regions to subcortical white matter, sparing subcortical U-fibers with absent or marked enhancement [1] (Fig. 9).

Several studies have identified fractional anisotropy maps derived from diffusion tensor imaging as a promising tool to investigate relations between white matter damage and

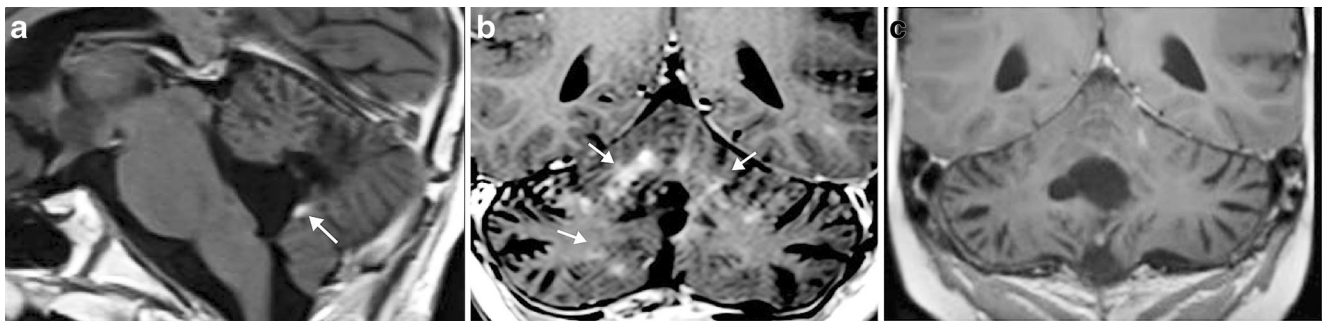


Fig. 8 Transient focal enhancing lesions in a 7-year-old boy with high-risk medulloblastoma. **a** Sagittal post-contrast T1-weighted sequence (TR/TE = 500 ms/9.9 ms, flip angle = 75°) obtained after surgery shows a small focus of contrast enhancement consistent with residual tumor (arrow). **b** Coronal post-contrast T1-weighted magnetization prepared rapid-acquisition gradient echo sequence (TR/TE/TI = 1,900/254/900 ms, flip angle = 9°) obtained 1 year after treatment initiation with

high-dose chemotherapy and hyper-fractionated accelerated radiotherapy shows areas of patchy focal contrast enhancement (arrows). **c** Coronal post-contrast T1-weighted sequence (TR/TE = 500/9.9 ms, flip angle = 75°) obtained 2 years after treatment initiation demonstrates almost complete disappearance of contrast-enhanced lesions. TE echo time, TI inversion time, TR repetition time

cognitive impairment associated with treatment-related toxicity. Studies on survivors of acute lymphoblastic leukemia and medulloblastomas found (1) significant differences between fractional anisotropy values in normal-appearing white matter tracts of patients compared to controls and (2) a statistical correlation between fractional anisotropy value abnormalities and neurocognitive test outcomes, suggesting an impaired microstructural anatomical substrate to altered cognition [50–53].

Recently with the introduction of the aforementioned therapeutic strategies developed for high-risk malignant central nervous system tumors, treatment-induced diffuse leukoencephalopathy has been reported, with subacute rather than chronic onset associated with devastating neurological

deficits. This condition has been reported with conflicting and in some cases warning percentages, especially in patients treated with thiotepa after hyperfractionated accelerated radiotherapy, suggesting a possible compounding effect of these therapies and raising the need for international multicenter clinical trials [45, 47, 54, 55] (Fig. 10).

Specific medication-related neurotoxicities

Methotrexate-induced neurotoxicity

Methotrexate is a component of chemotherapy for acute lymphoblastic leukemia and has been recognized to be the main

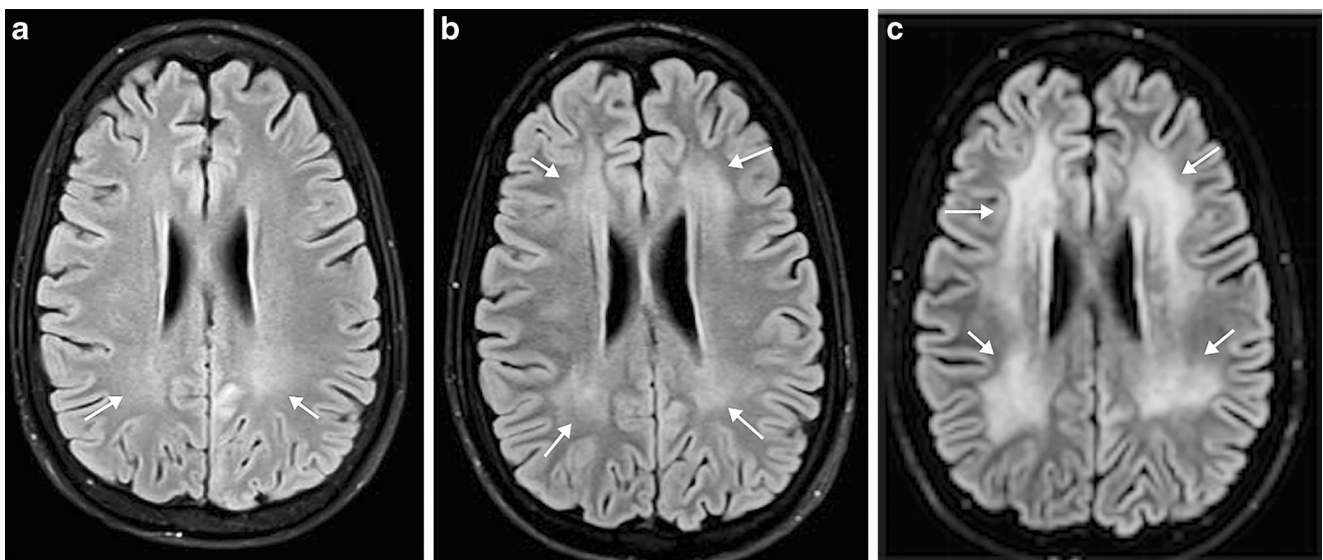


Fig. 9 Progressive leukoencephalopathy in a 15-year-old boy with acute lymphoblastic leukemia treated with chemotherapy. **a** Axial FLAIR sequence (TR/TE/TI = 9,000/85/500 ms, flip angle = 150°) from MRI examination performed 3 years after treatment initiation demonstrates presence of confluent periventricular white matter hyperintensities

following a centrifugal pattern with sparing of U-fibers (arrows). **b, c** Same MRI sequence at 5-year follow-up (**b**) and at 6-year follow-up (**c**) shows progressive and symmetrical increased extension of signal alterations (arrows). FLAIR fluid-attenuated inversion recovery, TE echo time, TI inversion time, TR repetition time

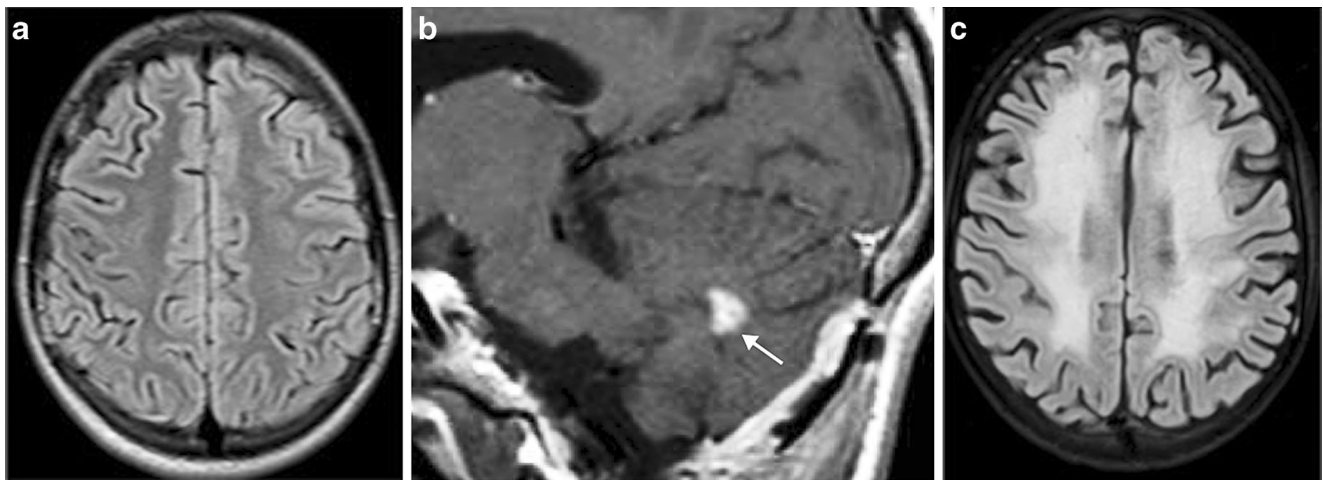


Fig. 10 Diffuse white matter injury in a 9-year-old boy with high-risk medulloblastoma treated with high-dose chemotherapy, hyperfractionated accelerated radiotherapy and two myeloablative courses of thiotepa with stem cell rescue. **a** After-treatment axial FLAIR MR sequence (TR/TE/TI = 9,000/85/500 ms, flip angle = 150°) shows absent signal alterations in the supratentorial compartment. **b** Sagittal post-contrast T1-weighted sequence (TR/TE = 500/9.9 ms, flip angle = 75°) demonstrates a small nodule of contrast enhancement

within the surgical cavity in the cerebellar region, suggestive of residual tumor (*arrow*). Two months after a myeloablative course of thiotepa, the boy experienced acute paraparesis and cognitive impairment. **c** Axial FLAIR MR sequence (TR/TE/TI = 9,000/85/500 ms, flip angle = 150°) demonstrates diffuse hyperintense signal involving supratentorial white matter. *FLAIR* fluid-attenuated inversion recovery, *TE* echo time, *TI* inversion time, *TR* repetition time

component responsible for acute therapy-induced neurotoxicity in children with acute lymphoblastic leukemia. Methotrexate inhibits cell replication by blocking the enzyme dihydrofolate reductase, thus preventing the conversion of folic acid to tetrahydrofolic acid. As it crosses the blood–brain barrier, it can be administered both intravenously and via intrathecal route to treat the disease and prevent recurrence in the central nervous system. The exact pathophysiological mechanisms of methotrexate-induced neurotoxicity are unclear, but both indirect (accumulation of adenosine and homocysteine) and direct (excitatory effect on N-methyl-D-aspartate receptors) toxic effects on brain tissue have been proposed [56]. Risk factors for toxicity include high-dose chemotherapy, intrathecal administration, associated brain radiation and young age [3].

Brain alterations related to methotrexate administration have been described as acute or chronic. The former are clinically characterized by stroke-like symptoms as aphasia, sensory deficits, ataxia and seizures, and have been more related to intrathecal administration [57]. On the other hand, chronic neurological effects, mainly consisting of cognitive disorders, have been more frequently associated with methotrexate intravenous injections [58, 59]. These differences are also reflected in the neuroradiologic findings. The neuroradiologic picture of acute methotrexate-induced toxicity is similar to that of acute toxic leukoencephalopathy (and these sometimes overlap), with bilateral hyperintensities on T2-weighted MR sequences within periventricular white matter and centrum semiovale, associated with foci of diffusion restriction in early phases, representing cytotoxic edema, probably the result of a direct neurotoxic effect of methotrexate on the cells (Fig. 11) [3, 57]. However regions of

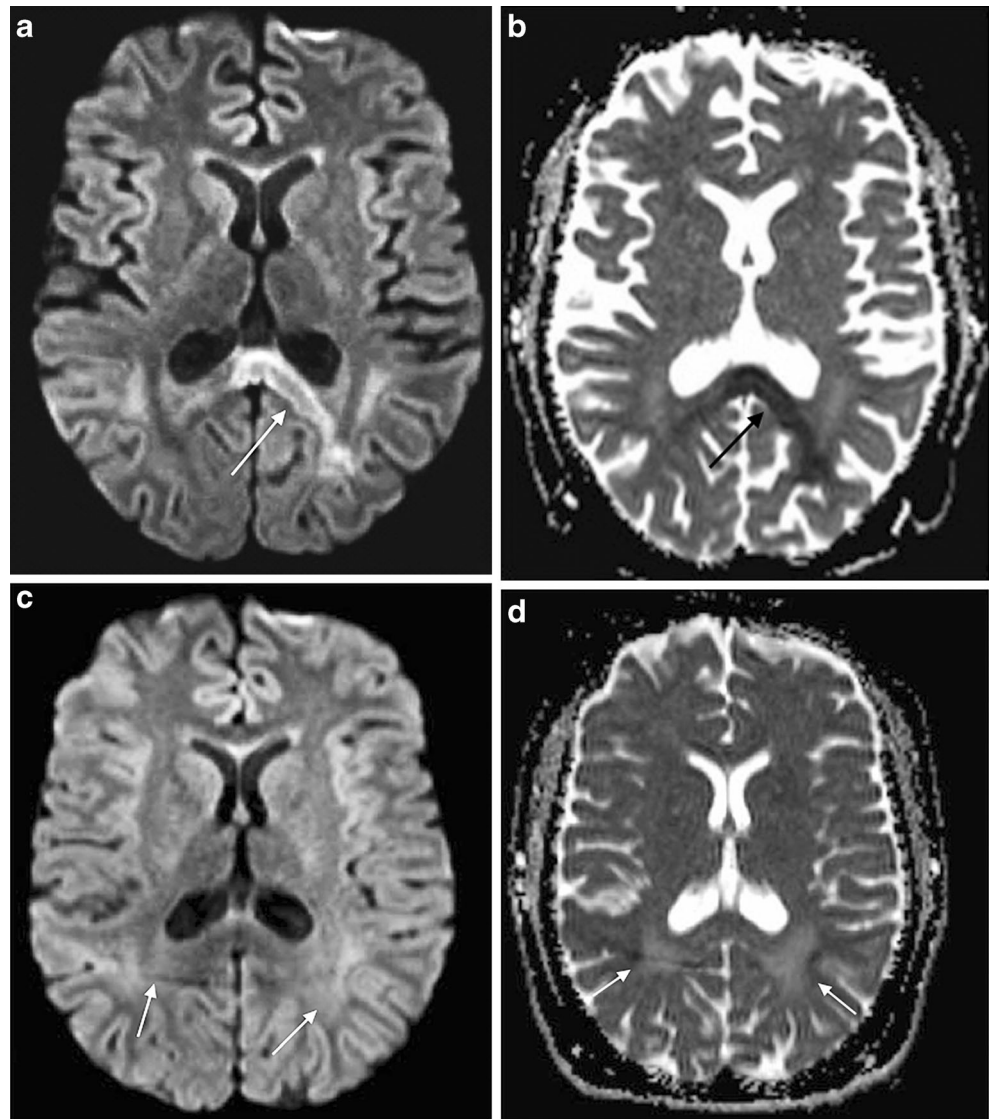
diffusion restriction after intrathecal administration of methotrexate are not necessarily associated with irreversible brain damage and cell death and, therefore, they should not worsen the prognosis [56, 57].

If compared to acute toxic leukoencephalopathy resulting from other medications, the neurotoxicity pattern related to methotrexate administration often shows involvement of the splenium of the corpus callosum (Fig. 11) [60]. After intravenous administration of methotrexate, the MRI pattern of neurotoxicity corresponds to a diffuse periventricular leukoencephalopathy, which is highly nonspecific, as already shown in concomitant chemotherapy- and radiotherapy-related findings. This pattern has been reported to occur in 9–33% of patients treated for acute lymphoblastic leukemia and intravenous methotrexate and never exposed to radiotherapy. However radiologic findings (in terms of extent and intensity of leukoencephalopathy) have shown a decrease over time by about 1.5 years after completion of therapy, suggesting a partial reversibility of the drug-related effects on cerebral white matter [58, 59].

L-asparaginase-related complications

L-asparaginase is an important component of remission-induction therapy in children affected by acute lymphoblastic leukemia. By hydrolyzing asparagine to aspartic acid and ammonia, L-asparaginase acts on different proteins throughout the body and can also affect the blood coagulation system. The most serious brain complications related to this treatment are indeed hemorrhagic and thromboembolic events resulting from L-asparaginase-induced alterations in the clotting system [61, 62].

Fig. 11 Methotrexate-associated neurotoxicity in a 10-year-old girl with acute lymphoblastic leukemia treated with chemotherapy and intrathecal methotrexate. After 2 months of methotrexate treatment, the girl experienced sudden headache, diplopia and left superior arm weakness. **a, b** An area of diffusion restriction (*arrow*) involving the splenium of the corpus callosum is shown on **(a)** axial diffusion-weighted MR image (TR/TE = 9,000/98 ms, b value = 1,000) and **(b)** corresponding apparent diffusion coefficient map (b values = 0, 1,000). **c, d** The same sequences performed at 1-month follow-up demonstrate resolution of foci of reduced diffusivity, with presence of periventricular hyperintensities and increased diffusivity (*arrows*). TE echo time, TR repetition time



Cerebral venous thrombosis is an acute complication of the induction phase of leukemia treatment with L-asparaginase that is observed in about 30% of acute neurologic adverse events in children with acute lymphoblastic leukemia. Clinical suspicion of cerebral venous thrombosis can be guided by the presence of seizures, focal neurological deficits and features of raised intracranial pressure, including headache, vomiting and altered mental status [62]. However because clinical manifestations of cerebral venous thrombosis can be extremely variable, it is mandatory, in order to avoid missing the diagnosis, to evaluate the patient with urgent neuroimaging techniques (CT or MRI), with protocols specifically focused on typical signs of cerebral venous thrombosis.

In the event of sinus thrombosis, non-contrast CT can detect the hyperdensity of the thrombosed sinus. Contrast-enhanced CT might show a characteristic sign called

“empty delta,” which is represented by enhancement surrounding the thrombosed sinus. However contrast-enhanced CT does not exceed a sensitivity of 60% in the diagnosis of cerebral venous thrombosis [62].

MRI is much more sensitive than CT in evaluating cerebral venous thrombosis, especially for the detection of early parenchymal infarction. On conventional images, the thrombus is mainly identified on T1-weighted images, especially in the subacute phase, demonstrating a hyperintense signal, whereas T2*-weighted gradient echo sequence might help in the identification of the thrombosed vein, especially in isolated cortical vein thrombosis cases. The demonstration of a flow void in MR venography is considered to be the most specific diagnostic sign of cerebral venous thrombosis, with a high sensitivity even in the acute phase of thrombosis, during which the main MR characteristics are isointensity on T1-weighted and low signal intensity on T2-weighted imaging [63, 64].

Vigabatrin-associated neurotoxicity

Vigabatrin is a selective and irreversible γ -aminobutyric acid transaminase inhibitor used as an anti-epileptic drug for the treatment of infantile spasms and refractory complex partial seizures in children and adults. The safety of vigabatrin was first challenged in a report of white matter anomalies from preclinical studies in rats, showing cellular vacuolation and intramyelic edema, but these results have not been demonstrated in humans [64, 65].

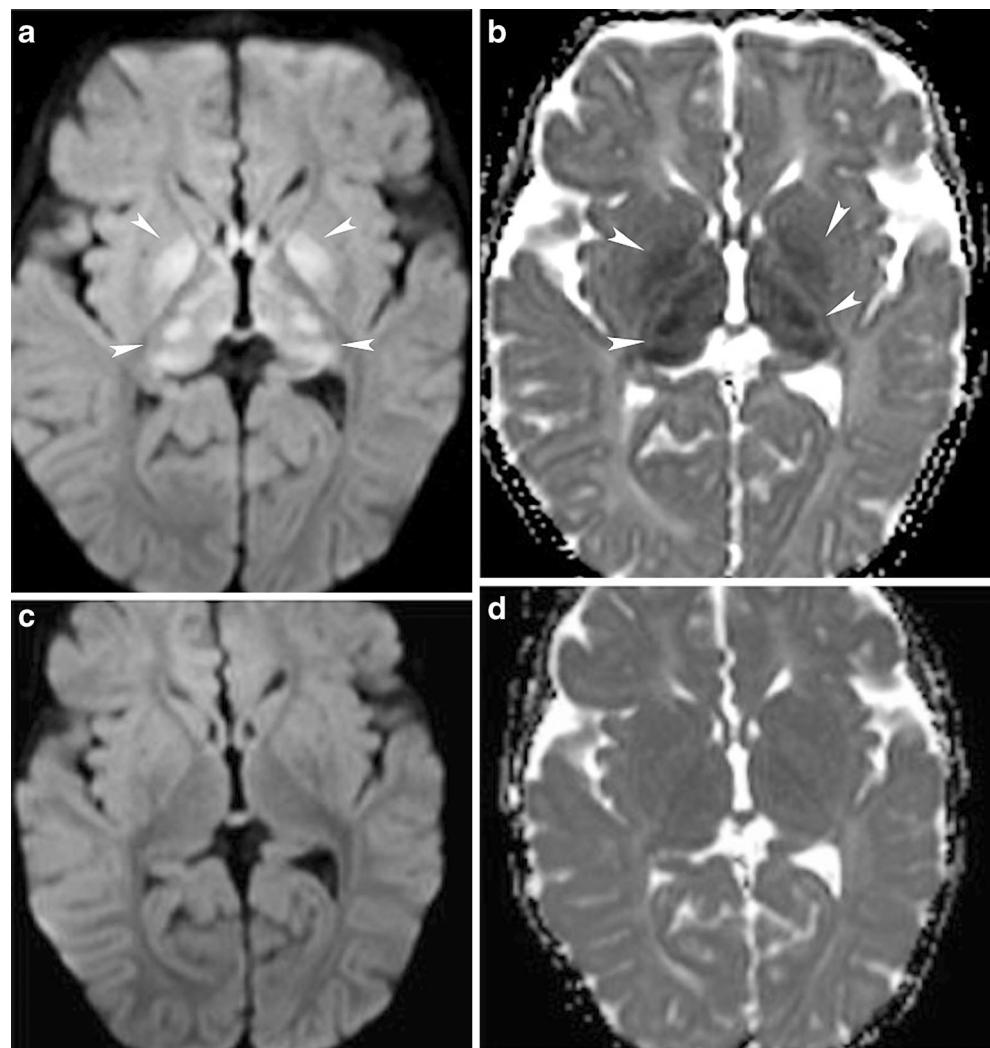
In young children with infantile spasms, high-dose vigabatrin administration might be associated with neurotoxicity, with transient asymptomatic MRI abnormalities in 10–20% of treated patients [64]. These alterations have been related mainly to vigabatrin administration rather than the underlying epileptic condition [66], and might be related to a γ -aminobutyric-acid-induced excitotoxicity mechanism, which provokes transient failure of the sodium/potassium adenosine triphosphate pump or

possibly transient cellular vacuolation, a result of depolarizing effects [65].

The MR pattern is characterized by the preferential involvement of deep brain structures, which, like the metronidazole-associated toxicity described in the next section, mainly affects the basal ganglia, corpus callosum, dentate nuclei and brainstem; more rarely, cerebellum and thalamus are affected. This distribution likely reflects a selective vulnerability to vigabatrin related to region-specific γ -aminobutyric acid metabolism [65].

On conventional imaging, brain lesions show high signal intensity on T2-weighted images, with restricted diffusion on diffusion-weighted imaging and apparent diffusion coefficient maps, a consequence of cytotoxic edema (Fig. 12). Usually these anomalies are transient, showing spontaneous resolution (without medication discontinuation) in about 12 months, and they have not been associated with any clinical sequelae, often remaining asymptomatic and with a good seizure control [3, 64, 65].

Fig. 12 Vigabatrin-related neurotoxicity in a 9-month-old girl with epileptic seizures. **a** Axial diffusion-weighted MR image (TR/TE = 9,000/98 ms, b value = 1,000) and **(b)** corresponding apparent diffusion coefficient map (b values = 0, 1,000) show areas of restricted diffusion (*arrowheads*) involving the globus pallidus and thalamus bilaterally and symmetrically, consistent with cytotoxic edema. **c, d** The same sequences obtained at follow-up MRI scan 2 months after therapy discontinuation demonstrate complete resolution of the neurotoxic pattern. *TE* echo time, *TR* repetition time



Consequently when toxic-related brain alterations are detected, vigabatrin administration can be continued under MRI surveillance.

Metronidazole neurotoxicity

Metronidazole is an antibiotic agent often used for the treatment of aerobic and protozoal infections. Therapy with high doses (more than 2 g per day) and for long periods, or in children with hepatic failure, can induce neurotoxicity, the pathogenic mechanism of which is still not entirely understood [67, 68].

Metronidazole neurotoxicity is clinically characterized by severe neurological symptoms such as cerebellar signs (ataxia, dysarthria), peripheral neuropathy, seizures and encephalopathy. MR anomalies involve deep brain structures such as cerebellar dentate nuclei, splenium of the corpus callosum, basal ganglia and brainstem [69]. The dentate nuclei involvement in children might depend on several pathological conditions (e.g., metabolic conditions, mitochondrial disorders, neurofibromatosis) that have to be taken into account in the differential diagnosis [70].

The most representative MR findings are T2 hyperintensities associated with high signal on apparent diffusion coefficient maps, indicating increased diffusion, which reflects vasogenic edema. However diffusion restriction has also been observed in acute phases, particularly within red nuclei and periaqueductal gray, showing the so-called “giant panda face with bright eyes” sign [70].

Some studies report that vasogenic edema predominates in cerebellar, midbrain and brainstem lesions, whereas cytotoxic edema prevails at supratentorial sites such as the corpus callosum and subcortical white matter [69]. MR

spectroscopy abnormalities have also been described in association with metronidazole use, namely the presence of a nonspecific elevated lactate peak. Typically complete resolution of neural tissue alterations on MR imaging is observed several weeks after discontinuing therapy.

Hepatic encephalopathy

Treatment-related liver toxicity is not an infrequent condition in children, and it may indirectly lead to subsequent neurological effects. The pathogenesis of hepatic encephalopathy might be explained by blood-accumulation of several compounds — namely manganese and ammonia — that are normally metabolized by a healthy liver but accumulate in cases of liver dysfunction. Manganese can be found in all human tissues and is metabolized by the liver and excreted via the hepatobiliary route. In children with liver failure, manganese concentration increases in plasma and enters the brain through the blood–brain barrier, developing a neurotoxic effect. Manganese neural deposition in children has been associated with food supplements, water pollution and parenteral nutrition (direct deposition), and can also be related to pharmacological therapy, depending on liver toxicity (indirect deposition) [71]. The clinical correlate varies from an asymptomatic condition to neurological symptoms including movement disorders and seizures, some of which might resolve after discontinuation of manganese supplementation or restoration of normal liver function [72, 73].

The primary brain region involved in manganese deposition is the basal ganglia, especially within the globus pallidus and striatum, which might show symmetrical hyperintensities on unenhanced T1-weighted MR sequences because of manganese’s paramagnetic properties

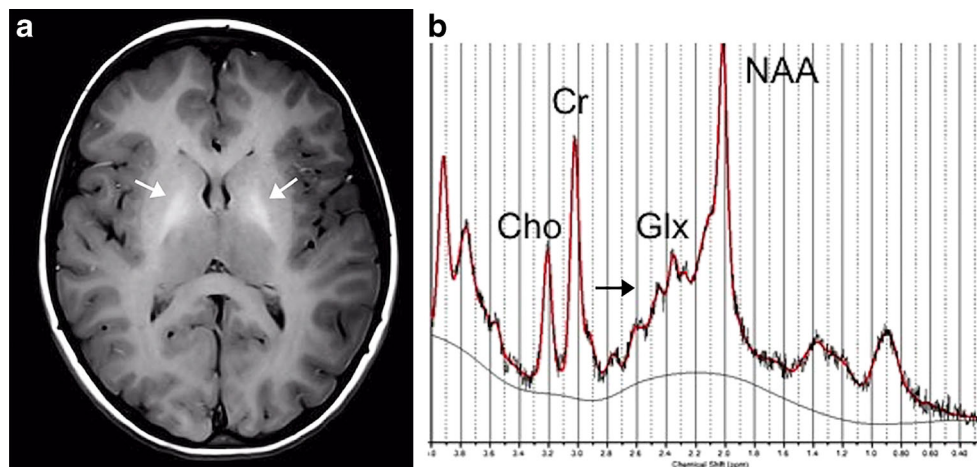


Fig. 13 Hepatic encephalopathy in an 8-year-old boy with primary biliary cirrhosis. **a** Axial T1-weighted sequence (TR/TE = 500/9.9 ms, flip angle = 75°) shows high signal intensity involving the globus pallidus bilaterally and symmetrically (arrows). **b** 1H MR spectroscopy water-suppressed proton spectra recorded with a stimulated echo acquisition mode pulse sequence (TR/TE = 1,500/30 ms;

acquisitions = 96) of a voxel located in the globus pallidus demonstrates an increase in the glutamine/glutamate region (Glx, 2.1–2.5 ppm, arrow). Other main resonances correspond to N-acetylaspartate (NAA, 2.0 ppm), creatine/phosphocreatine (Cr, 3.02 ppm) and choline-containing compounds (Cho, 3.2 ppm). TE echo time, TR repetition time

[72]. In case of liver failure, elevated levels of circulating ammonia can be detected in blood and are sometimes deposited in brain tissue, passing through the blood–brain barrier. This deposit can induce high glutamine levels and astrocytes swelling as a result of ammonia detoxification, finally leading to brain edema and increased intracranial pressure. In cases of hepatic encephalopathy, MR spectroscopy studies show an increase in the glutamine/glutamate signal intensity accompanied by myoinositol depletion and a decrease in the choline signal intensity, a result of ammonia metabolic pathway (Fig. 13) [71].

Conclusion

Neurotoxicity in children can be the result of many disease treatments, often leading to life-threatening clinical conditions. Considering the complexity of therapeutic protocols used in the pediatric oncologic–hematologic population, and the individual susceptibility to neurotoxic damage, it is extremely important to consider the suggested categories of neurotoxic conditions as a continuous spectrum of overlapping clinical and radiologic scenarios, and not as categories confined in a rigid scheme. The knowledge of treatment protocols, modalities of administration and therapeutic timelines with special attention to specific MRI patterns of neurotoxicity might be conducive to prompt recognition and a multidisciplinary approach encompassing continual communication among oncologists, radiotherapists and radiologists, all of which is of paramount importance for the child's correct diagnostic and therapeutic management.

Compliance with ethical standards

Conflicts of interest None

References

1. Pružincová E, Šteňo J, Srbecký M et al (2009) MR imaging of late radiation therapy- and chemotherapy-induced injury: a pictorial essay. *Eur Radiol* 19:2716–2727
2. Ball WS Jr, Prenger EC, Ballard ET (1992) Neurotoxicity of radio/chemotherapy in children: pathologic and MR correlation. *AJNR Am J Neuroradiol* 13:761–776
3. Iyer RS, Chaturvedi A, Pruthi S et al (2011) Medication neurotoxicity in children. *Pediatr Radiol* 41:1455–1464
4. Vázquez E, Lucaya J, Castellote A et al (2002) Neuroimaging in pediatric leukemia and lymphoma: differential diagnosis. *Radiographics* 22:1411–1428
5. Vázquez E, Delgado I, Sánchez-Montañez A et al (2011) Side effects of oncologic therapies in the pediatric central nervous system: update on neuroimaging findings. *Radiographics* 31:1123–1139
6. Valk J, Van der Knaap S (1992) Toxic encephalopathy. *AJNR Am J Neuroradiol* 13:747–760
7. Reddick WE, Taghipour DJ, Glass JO et al (2014) Prognostic factors that increase the risk for reduced white matter volumes and deficits in attention and learning for survivors of childhood cancers. *Pediatr Blood Cancer* 61:1074–1079
8. Oeffinger K, Mertens A, Sklar C et al (2006) Chronic health conditions in adult survivors of childhood cancer. *N Engl J Med* 355:1572–1582
9. Hudson MM, Ness KK, Gurney JG et al (2013) Clinical ascertainment health outcomes among adults treated for childhood cancer. *JAMA* 309:2371–2381
10. Quattrocchi CC, Errante Y, Rossi Espagnet MC (2016) Magnetic resonance imaging differential diagnosis of brainstem lesions in children. *World J Radiol* 8:1–20
11. Greene-Schloesser D, Robbins ME, Peiffer AM et al (2012) Radiation-induced brain injury: a review. *Front Oncol* 19:2–73
12. Perry A, Schmidt RE (2006) Cancer therapy-associated CNS neuropathology: an update and review of the literature. *Acta Neuropathol* 111:197–212
13. O'Brien BJ, Coleen RR (2014) Post-treatment imaging changes in primary brain tumors. *Curr Oncol Rep* 16:397
14. Murphy ES, Merchant TE, Wu S et al (2012) Necrosis after craniospinal irradiation: results from a prospective series of children with central nervous system embryonal tumors. *Int J Radiat Oncol Biol Phys* 83:e655–e660
15. Kumar AJ, Leeds NE, Fuller GN et al (2000) Malignant gliomas: MR imaging spectrum of radiation therapy- and chemotherapy-induced necrosis of the brain after treatment. *Radiology* 217:377–384
16. Poussaint TY, Rodriguez D (2006) Advanced neuroimaging of pediatric brain tumors: MR diffusion, MR perfusion, and MR spectroscopy. *Neuroimaging Clin N Am* 16:169–192
17. Ball WS, Holland SK (2001) Perfusion imaging in the pediatric patient. *Magn Reson Imaging Clin N Am* 9:207–230
18. Bangiyev L, Rossi Espagnet MC, Young R (2014) Adult brain tumor imaging: state of the art. *Semin Roentgenol* 49:39–52
19. Sugahara T, Korogi Y, Tomiguchi S et al (2000) Post-therapeutic intraaxial brain tumor: the value of perfusion-sensitive contrast-enhanced MR imaging for differentiating tumor recurrence from nonneoplastic contrast-enhancing tissue. *AJNR Am J Neuroradiol* 21:901–909
20. Hu LS, Baxter LC, Smith KA et al (2009) Relative cerebral blood volume values to differentiate high-grade glioma recurrence from post-treatment radiation effect: direct correlation between image-guided tissue histopathology and localized dynamic susceptibility-weighted contrast-enhanced perfusion MR imaging measurements. *AJNR Am J Neuroradiol* 30:552–558
21. Verma N, Cowperthwaite MC, Burnett MG et al (2013) Differentiating tumor recurrence from treatment necrosis: a review of neuro-oncologic imaging strategies. *Neuro Oncol* 15:515–534
22. Merchant T, Farr JB (2014) Proton beam therapy: a fad or a new standard of care. *Curr Opin Pediatr* 26:3–8
23. Faraci M, Morana G, Bagnasco F et al (2011) Magnetic resonance imaging in childhood leukemia survivors treated with cranial radiotherapy: a cross sectional, single center study. *Pediatr Blood Cancer* 57:240–246
24. Koike T, Yanagimachi N, Ishiguro H et al (2012) High incidence of radiation-induced cavernous hemangioma in long-term survivors who underwent hematopoietic stem cell transplantation with radiation therapy during childhood or adolescence. *Biol Blood Marrow Transplant* 18:1090–1098
25. Huisman TAGM, Singhi S, Pinto PS (2010) Non-invasive imaging of intracranial pediatric vascular lesions. *Childs Nerv Syst* 26:1275–1295
26. Di Giannatale A, Morana G, Rossi A et al (2014) Natural history of cavernous malformations in children with brain tumors treated with radiotherapy and chemotherapy. *J Neuro Oncol* 117:311–320

27. Nimjee SM, Powers CJ, Bulsara KR (2004) Review of the literature on de novo formation of cavernous malformations of the central nervous system after radiation therapy. *Neurosurg Focus* 21:e4
28. Acciarri N, Galassi E, Giulioni M et al (2009) Cavernous malformations of the central nervous system in the pediatric age group. *Pediatr Neurosurg* 45:81–104
29. Chen CY, Zimmerman RA, Faro S et al (1996) Childhood leukemia: central nervous system abnormalities during and after treatment. *AJNR Am J Neuroradiol* 17:295–310
30. Löning L, Zimmermann M, Reiter A et al (2000) Secondary neoplasms subsequent to Berlin-Frankfurt-Münster therapy of acute lymphoblastic leukemia in childhood: significantly lower risk without cranial radiotherapy. *Blood* 95:2770–2775
31. Hijjiya N, Hudson MM, Lensing S et al (2007) Cumulative incidence of secondary neoplasms as a first event after childhood acute lymphoblastic leukemia. *JAMA* 297:1207–1215
32. Bartynski WS (2008) Posterior reversible encephalopathy syndrome, part 1: fundamental imaging and clinical features. *AJNR Am J Neuroradiol* 29:1036–1042
33. Morris EB, Laningham FH, Sandlund JT et al (2007) Posterior reversible encephalopathy syndrome in children with cancer. *Pediatr Blood Cancer* 48:152–159
34. Bartynski WS (2008) Posterior reversible encephalopathy syndrome, part 2: controversies surrounding pathophysiology of vasogenic edema. *AJNR Am J Neuroradiol* 29:1043–1049
35. Patel AJ, Fox BD, Fulkerson DH et al (2010) Posterior reversible encephalopathy syndrome during posterior fossa tumor resection in a child. *J Neurosurg Pediatr* 6:377–380
36. Hodnett P, Coyle J, O'Regan K et al (2009) PRES (posterior reversible encephalopathy syndrome), a rare complication of tacrolimus therapy. *Emerg Radiol* 16:493–496
37. Donmez FY, Guleryuz P, Agildere M (2014) MRI findings in childhood PRES: what is different than the adults? *Clin Neuroradiol* 26:209–213
38. McKinney AM, Short J, Truwit CL et al (2007) Posterior reversible encephalopathy syndrome: incidence of atypical regions of involvement and imaging findings. *AJR Am J Roentgenol* 189:904–912
39. McKinney AM, Kieffer SA, Paylor RT et al (2009) Acute toxic leukoencephalopathy: potential for reversibility clinically and on MRI with diffusion-weighted and FLAIR imaging. *AJR Am J Roentgenol* 193:192–206
40. Filley CM, Kleinschmidt-DeMasters BK (2001) Toxic leukoencephalopathy. *N Engl J Med* 345:425–432
41. Akiba T, Okeda R, Tajima T (1996) Metabolites of 5-fluorouracil, alpha-fluoro-beta-alanine and fluoroacetic acid, directly injure myelinated fibers in tissue culture. *Acta Neuropathol* 92:8–13
42. Wijdicks EF (2001) Neurotoxicity of immunosuppressive drugs. *Liver Transpl* 7:937–942
43. Beitinjaneh A, McKinney AM, Cao Q et al (2011) Toxic leukoencephalopathy following fludarabine-associated hematopoietic cell transplantation. *Biol Blood Marrow Transplant* 17:300–308
44. Gandola L, Massimino M, Cefalo G et al (2009) Hyperfractionated accelerated radiotherapy in the Milan strategy for metastatic medulloblastoma. *J Clin Oncol* 27:566–571
45. Vivekanandan S, Breene R, Ramanujachar R et al (2015) The UK experience of a treatment strategy for pediatric metastatic medulloblastoma comprising intensive induction chemotherapy, hyperfractionated accelerated radiotherapy and response directed high dose myeloablative chemotherapy or maintenance chemotherapy (Milan strategy). *Pediatr Blood Cancer* 62:2132–2139
46. Spreafico F, Gandola L, Marchianò A et al (2008) Brain magnetic resonance imaging after high-dose chemotherapy and radiotherapy for childhood brain. *Int J Radiat Oncol Biol Phys* 70:1011–1019
47. Thust SC, Blanco E, Michalski AJ et al (2014) MRI abnormalities in children following sequential chemotherapy, hyperfractionated accelerated radiotherapy and high-dose thiotepa for high-risk primitive neuroectodermal tumours of the central nervous system. *J Med Imaging Radiat Oncol* 58:683–690
48. Fouladi M, Chintagumpala M, Laningham FH et al (2004) White matter lesions detected by magnetic resonance imaging after radiotherapy and high-dose chemotherapy in children with medulloblastoma or primitive neuroectodermal tumor. *J Clin Oncol* 22:4551–4560
49. Dietrich U, Wanke I, Mueller T et al (2001) White matter disease in children treated for malignant brain tumors. *Childs Nerv Syst* 17:731–738
50. Edelmann MN, Krull KR, Liu W et al (2014) Diffusion tensor imaging and neurocognition in survivors of childhood acute lymphoblastic leukaemia. *Brain* 137:2973–2983
51. Khong PL, Leung LH, Chan GC et al (2005) White matter anisotropy in childhood medulloblastoma survivors: association with neurotoxicity risk factors. *Radiology* 236:647–652
52. Khong PL, Leung LH, Fung AS et al (2006) White matter anisotropy in post-treatment childhood cancer survivors: preliminary evidence of association with neurocognitive function. *J Clin Oncol* 24:884–890
53. Palmer SL, Reddick WE, Glass JO et al (2010) Regional white matter anisotropy and reading ability in patients treated for pediatric embryonal tumors. *Brain Imaging Behav* 4:132–140
54. Massimino M, Spreafico F, Pignoli E et al (2016) Comment on: The UK experience of a treatment strategy for pediatric metastatic medulloblastoma comprising intensive induction chemotherapy, hyperfractionated accelerated radiotherapy and response directed high-dose myeloablative chemotherapy or maintenance chemotherapy (Milan strategy). *Pediatr Blood Cancer* 63:1123–1124
55. Vivekanandan S (2016) Reply to comment on: The UK experience of a treatment strategy for pediatric metastatic medulloblastoma comprising intensive induction chemotherapy, hyperfractionated accelerated radiotherapy, and response-directed high-dose myeloablative chemotherapy or maintenance chemotherapy (Milan strategy). *Pediatr Blood Cancer* 63:1125–1126
56. Fisher MJ, Khademian ZP, Simon EM et al (2005) Diffusion-weighted MR imaging of early methotrexate-related neurotoxicity in children. *AJNR Am J Neuroradiol* 26:1686–1689
57. Rollins N, Winick N, Bash R et al (2004) Acute methotrexate neurotoxicity: findings on diffusion-weighted imaging and correlation with clinical outcome. *AJNR Am J Neuroradiol* 25:1688–1695
58. Reddick WE, Glass JO, Helton KJ et al (2005) Prevalence of leukoencephalopathy in children treated for acute lymphoblastic leukemia with high-dose methotrexate. *AJNR Am J Neuroradiol* 26:1263–1269
59. Reddick WE, Glass JO, Helton KJ et al (2005) A quantitative MR imaging assessment of leukoencephalopathy in children treated for acute lymphoblastic leukemia without irradiation. *AJNR Am J Neuroradiol* 26:2371–2377
60. Sandoval C, Kutscher M, Jayabose S et al (2003) Neurotoxicity of intrathecal methotrexate: MR imaging findings. *AJNR Am J Neuroradiol* 24:1887–1890
61. Schulz U, Mann G, Zoubek A et al (1994) Venous thrombosis of cranial sinuses in asparaginase therapy: a case report. *Klin Padiatr* 206:342–345
62. Wani NA, Kosar T, Pala NA et al (2010) Sagittal sinus thrombosis due to L-asparaginase. *J Pediatr Neurosci* 5:32–35
63. Boukobza M, Crassard I, Bousser MG et al (2009) MR imaging features of isolated cortical vein thrombosis: diagnosis and follow-up. *AJNR Am J Neuroradiol* 30:344–348
64. Wheelless JW, Carmant L, Bebin M et al (2009) Magnetic resonance imaging abnormalities associated with vigabatrin in patients with epilepsy. *Epilepsia* 50:195–205
65. Pearl PL, Vezina LG, Saneto RP et al (2009) Cerebral MRI abnormalities associated with vigabatrin therapy. *Epilepsia* 50:184–194

66. Milh M, Villeneuve N, Chapon F et al (2009) Transient brain magnetic resonance imaging hyperintensity in basal ganglia and brain stem of epileptic infants treated with vigabatrin. *J Child Neurol* 24:305–315
67. Frytak S, Moertel CH (1978) Childs DS neurologic toxicity associated with high-dose metronidazole therapy. *Ann Intern Med* 88:361–362
68. Heaney CJ, Campeau NG, Lindell EP (2003) MR imaging and diffusion-weighted imaging changes in metronidazole (Flagyl)-induced cerebellar toxicity. *AJNR Am J Neuroradiol* 24:1615–1617
69. Kim E, Na DG, Kim EY et al (2007) MR imaging of metronidazole-induced encephalopathy: lesion distribution and diffusion-weighted imaging findings. *AJNR Am J Neuroradiol* 28:1652–1658
70. McErlean A, Abdalia K, Donoghue V et al (2010) The dentate nucleus in children: normal development and patterns of disease. *Pediatr Radiol* 40:326–339
71. Rovira A, Alonso J, Córdoba J (2008) MR imaging findings in hepatic encephalopathy. *AJNR Am J Neuroradiol* 29:1612–1621
72. Aschner J, Anderson A, Slaughter J et al (2015) Neuroimaging identifies increased manganese deposition in infants receiving parenteral nutrition. *Am J Clin Nutr* 102:1482–1489
73. Jiang J, Shi S, Zhou Q et al (2014) Downregulation of the Wnt/ β -catenin signaling pathway is involved in manganese-induced neurotoxicity in rat striatum and PC12 cells. *J Neurosci Res* 92:783–794